Physica B 406 (2011) 4333–4337

Contents lists available at SciVerse ScienceDirect

Physica B

journal homepage: www.elsevier.com/locate/physb

# Magnetic entropy change in perovskite manganites $La_{0.6}Pr_{0.1}Pb_{0.3}MnO_3$ with double metal–insulator peaks

Zhiming Wang [a,c,*], Qingyu Xu [b], Gang Ni [d], He Zhang [a]

[a] Institute of Mechanical Engineering, Nanjing University of Science and Technology, Nanjing 210094, PR China
[b] Department of Physics, Southeast University, Nanjing 211189, China
[c] National Laboratory of Solid State Microstructures, Nanjing University, Nanjing 210093, China
[d] Department of Physics Fudan University, Shanghai 200433, China

ARTICLE INFO

*Article history:*
Received 6 May 2011
Received in revised form
27 July 2011
Accepted 4 August 2011
Available online 30 August 2011

*Keywords:*
Perovskite manganite
Double metal-insulator peaks
Magnetic entropy change

ABSTRACT

Following the double metal–insulator peaks found in series of perovskite manganites $La_{0.7-x}Pr_xPb_{0.3}MnO_3$ ($x$=0, 0.05, 0.1), the magnetic entropy change of $La_{0.6}Pr_{0.1}Pb_{0.3}MnO_3$ was carefully investigated as a representative. The maximum magnetic entropy change ($\Delta S_H = -1.7$ J/kg K at 300 K) and the expanded refrigerant capacity (about 123.8 J/kg) had been obtained under 10 kOe magnetic field variation, though the double peak of maximum magnetic entropy change had not occurred since the comparative faint magnetic signal from the Pr ions inhomogeneity existed in the octahedral frame submerged in the strong magnetic signal originated from the dominating octahedral frame both in the double exchange mechanism, but the width at half maximum in the magnetic entropy change comparatively broadened.



## 1. Introduction

Recently, the perovskite manganites $Ln_{1-x}T_xMnO_3$ ($Ln^{3+}=La^{3+}$, $Pr^{3+}$, $Nd^{3+}$, $Sm^{3+}$, $Y^{3+}$, etc. $T^{2+}=Ca^{2+}$, $Sr^{2+}$, $Ba^{2+}$, $Pb^{2+}$, etc. $ABO_3$ type) had attracted considerable interest because they exhibit interesting physical effects and had potential applications due to the complex relationship between crystal structure, electrical, magnetic, and thermal properties, for example, the negative colossal magnetoresistance effect (CMR) and the common insulator–metal transition had been observed in the typical CMR material, the later generally accompanied by a Paramagnetic–Ferromagnetic transition [1–5].

Another important physical effect, the magnetocaloric effect, which results from the spin-ordering (i.e. ferromagnetic ordering) and is induced by the variation of the applied magnetic field, is crucial to the technology of magnetic refrigeration with many advantages over gas refrigeration: low noise, softer vibration, longer usage time, and absence of freon, etc. In perovskite manganites, the same with CMR, the magnetocaloric (MC) effect also are often observed around the Paramagnetic–Ferromagnetic transition temperature (i.e. the Curie temperature between a low-temperature, metallic–ferromagnetic state and a high-temperature, insulating–paramagnetic state) and this evidently suggests that there exists a certain of relation between the magnetic entropy change and the resistivity [6–8].

Following the discovered double metal–insulator peaks, the impetus for this paper study was seeking after the possible broad and large refrigerant capacity of the magnetocaloric effect in the perovskite manganites under conveniently low fields and at room temperature.

In the investigation about the perovskite manganites, most efforts had been focused on the doping range $x \sim 0.3$ or 0.33, which is an optimized percentage of $Mn^{3+}$ replaced with $Mn^{4+}$ for the electronic doping and providing potential charge carriers for the electronic conductivity in the double-exchange interaction, for the considerable perovskite manganites in the above-mentioned electronic doping range, these compounds are metallic and ferromagnetic at low temperature, while their conductivity displays the insulating or semiconducting behavior at high temperature. There is a transition between the low-temperature, metallic–ferromagnetic state and the high-temperature, insulating–paramagnetic state in which the magnetic ordering transition is incident with the metal–insulator transition [1–8].

The simultaneous occurrence of ferromagnetism and metallic behavior in perovskite manganites had been explained using the double exchange mechanism (DE), which involves interaction between pairs of $Mn^{3+}$ and $Mn^{4+}$ ions as proposed by Zener [9]. According to the model, $e_g$ electrons could transfer easily between ions if the manganese spins were on the alignments of some frame in the certain of temperature, pressure, applied magnetic field, etc. and then the resistivity behavior showed a metal–insulator (MI)

* Corresponding author at: Institute of Mechanical Engineering, Nanjing University of Science and Technology, Nanjing 210094, China.
Tel.: +86 25 84318429; fax: +86 25 84315694.
*E-mail address:* zhimingwang@mail.njust.edu.cn (Z. Wang).

0921-4526/$ - see front matter © 2011 Elsevier B.V. All rights reserved.
doi:10.1016/j.physb.2011.08.015

peak in some manganite samples. However, it was suggested that the double exchange mechanism alone was not sufficient to explain the details of the observed resistivity behavior such as the insulating behavior above $T_C$, here, the origin of the double resistivity peaks was still considered an open question and more investigations had to be carried out to elucidate their nature [10–17,23].

## 2. Experiments

The doped perovskite manganites $La_{0.7-x}Pr_xPb_{0.3}MnO_3$ ($x$=0, 0.05, 0.1) were prepared by sol–gel technique. Citric acid was used as a gelling agent for La, Pr, Pb, and Mn ions in a sand bath, and the obtained gel was subjected to successive heat treatment at 873 K for 2 h. After that, the microcrystalline powder was pelletized, pressed into disks and sintered at 1473 K for 24 h in an oxygen flow. The crystal structure of the bulk samples was determined by an X-ray diffractometer (XRD) with CuKα radiation (RK-D/Max-RA). Magnetization was measured using a vibrating sample magnetometer (VSM, LakeShore Cryotronics Inc.) with an absolute accuracy of $5\times10^{-5}$ emu, in which a sample was placed inside a polyethylene pipe. The magnetization of an isothermal regime in the series samples was measured under an applied magnetic field varying from 0 to 10 kOe. The isotherms $M$ vs $H$ measurement were performed from 150 K–350 K run-through the ferromagnetic ordering transition temperature ($T_C$) of a representative sample $La_{0.6}Pr_{0.1}Pb_{0.3}MnO_3$, the isothermal $M$–$H$ curves were obtained by step of 10 K. $M$–$H$ loops were measured at 160 K, 220 K, 275 K for the sample, respectively.

By conventional in-line four-probe technique, resistivity $\rho$ was measured as a function of temperature in a superconducting magnet with a maximum applied field of 1 T.

The MR was calculated according to the equation given below:

$$MR(\%)=\frac{\rho(0,T)-\rho(H,T)}{\rho(0,T)}\times 100\%$$

where $\rho(0,T)$ was the zero field resistivity and $\rho(H,T)$ was the resistivity under external magnetic field.

## 3. Results and discussions

Fig. 1 presented an X-ray pattern of sample $La_{0.6}Pr_{0.1}Pb_{0.3}MnO_3$ and indicated that single-phase perovskite manganites, and the peak corresponding to MnO, $MnO_2$, and $Mn_3O_4$ had not been observed [PDF number: 22-1123 wavelength 1.5418 Å]. Fig. 2 showed the electrical resistivity as a function of temperature for the $La_{0.6}Pr_{0.1}Pb_{0.3}MnO_3$ sample under 0 kOe and 10 kOe, respectively. Under

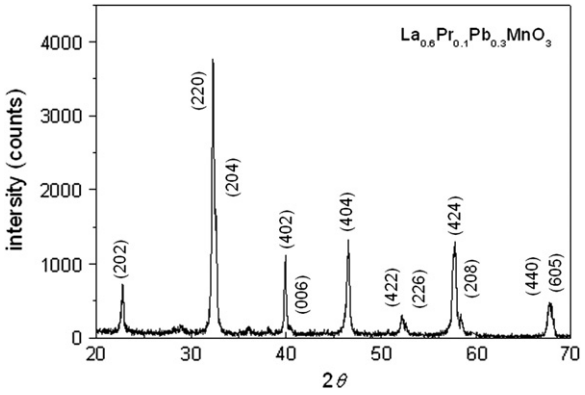


**Fig. 1.** Electrical resistivity as a function of temperature for the $La_{0.6}Pr_{0.1}Pb_{0.3}MnO_3$ sample under 0 kOe and 10 kOe, respectively. The inset showed the resistivity of $La_{0.7-x}Pr_xPb_{0.3}MnO_3$ ($x$=0, 0.05) samples under 0 kOe as a function of temperature.

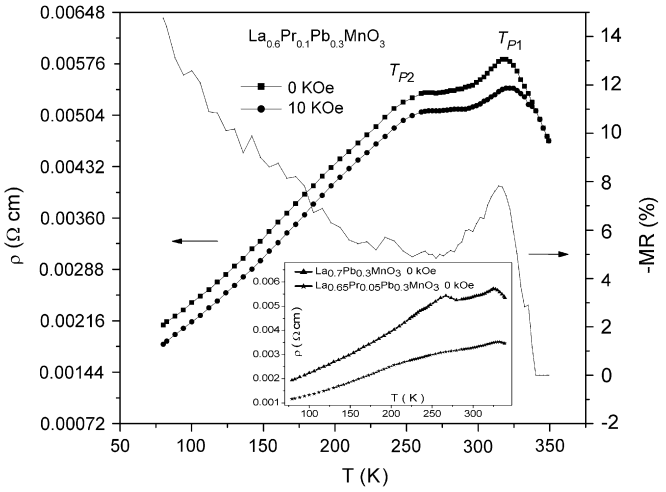


**Fig. 2.** X-ray diffraction pattern for the sample $La_{0.6}Pr_{0.1}Pb_{0.3}MnO_3$.

0 kOe, the $La_{0.6}Pr_{0.1}Pb_{0.3}MnO_3$ sample showed the double metal–insulator transition peaks where the first peak at 322 K is defined as $T_{p1}$ and the second peak, $T_{p2}$ at around 258 K. Under 10 kOe magnetic field, there was suppressed resistivity behavior in the sample $La_{0.6}Pr_{0.1}Pb_{0.3}MnO_3$, which is typical CMR behavior. The inset showed the resistivity of $La_{0.7-x}Pr_xPb_{0.3}MnO_3$ ($x$=0, 0.05) samples under 0 kOe as a function of temperature. Double metal–insulator peaks also occurred to these samples in the series.

With double M–I transition peaks $T_{p1}$ and $T_{p2}$, the perovskite samples was rather attractive to improve the magnetocaloric effect, in which double magnetic entropy change peaks or broaden magnetic entropy change were expected.

The shifting of $T_{p1}$ to slightly higher temperatures in the presence of external magnetic field (Fig. 2) might be due to increased alignment of magnetic moments causing delocalization of $e_g$ electrons and enhancement of DE interaction between $Mn^{3+}$ and $Mn^{4+}$. The delocalization was suggested to contribute to reduction of the $T_{p1}$ resistivity peak. In addition, the fact that the MR peak was present in the vicinity of $T_{p1}$ for $x$=0.1 $La_{0.6}Pr_{0.1}Pb_{0.3}MnO_3$ (Fig. 2) also indicated that the origin of both MR and $T_{p1}$ peaks were related to the same mechanism, which was based on the double exchange interactions.

However, the fact that the $T_{p2}$ peak did not shift in position upon application of external magnetic field indicated that the origin of this peak was different from that of the $T_{p1}$ peak. A previous study suggested that the secondary $T_{p2}$ peak originates from oxygen vacancies, valence states, ionic radii, external pressure, or magnetic inhomogeneity [18–23].

Uehara et al. [24] reported for the resistivity vs temperature at several Pr compositions of $La_{5/8-y}Pr_yCa_{3/8}MnO_3$ using electron microscopy techniques in 1999, that the rapid reduction with increasing $y$ of the temperature at which the peak occurs, which correlated with the Curie temperature, had been interpreted as the evidence of two-phase coexistence, involving a stable ferromagnetic state at small $y$, and a stable charge ordered (CO) state in the large $y$ PrCaMnO compound. Uehara et al. [24] finally substantiated their claims of phase separation, the direct evidence of the two-phase coexistence was provided by their Dark-field Images of electron microscopy. Using scanning tunneling spectroscopy, Fath et al. [25] had observed a clear phase-separated state in manganites $La_{1-x}Ca_xMnO_3$ and had reported the coexistence of metallic and insulating cluster clouds, based on the different spectroscopic signatures in the insulating (paramagnetic) and metallic (ferromagnetic) phases.

Billinge et al. [26] had lately studied the $MnO_6$ octahedral bond length distribution of $La_{1-x}Ca_xMnO_3$ using pair-distribution-function analysis of neutron powder-diffraction data, in the insulating phases the Jahn–Teller Mn–O long bond was clearly apparent, in the ferromagnetic phase Jahn–Teller Mn–O short bond was dominative, the pair-distribution-function analysis signifies the coexistence of charge localized (insulating) and delocalized phases (metallic) as the MI boundary was gradually approached.

The second M–I transition peaks might be due to existence of paramagnetic, ferromagnetic, and insulating, metallic clusters in the region below *T*c, which may also contribute to the conductivity and then $T_{p2}$ peak occurred [27]. Mixed ferromagnetic insulating and ferromagnetic metallic phases and $T_{p2}$ had also been observed for $La_{1-x}Cd_xMnO_3$ [28] and $La_{0.9-x}Sm_xTe_{0.2}MnO_3$ [29]. Furthermore, Electron Paramagnetic Resonance (ESR) studied on $La_{0.875}Sr_{0.125}MnO_3$ had indicated presence of mixed ferromagnetic insulating and ferromagnetic metallic phases below $T_c$ [30]. It could be concluded that the $T_{p2}$ peak was not due to impurity phases in the series samples, which was also approved by our XRD results.

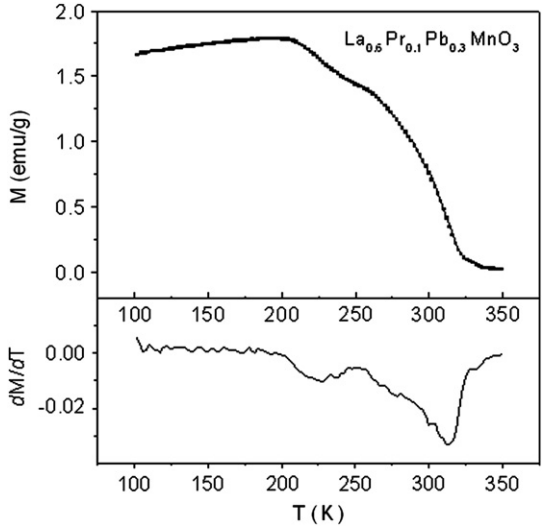


**Fig. 3.** Top plot showed temperature dependence at 50 Oe low field magnetization for sample $La_{0.6}Pr_{0.1}Pb_{0.3}MnO_3$. The base plot is the d*M*/d*T*–*T* curve from *M*–*T* curves, the Curie temperature $T_C$ had been determined from temperature at reaching a minimum.

The temperature dependence of low field magnetization for the two above-mentioned samples, shown in Fig. 3, was measured in a wide range of temperature (from 100 K up to 360 K) in 50 Oe applied field in order to determine the transition temperature of the material. The ferromagnetic ordering transition temperature $T_C$, defined as the temperature at which the d*M*/d*T*–*T* curve reaches a minimum, had been determined from *M*–*T* curves. From several segment characteristics of *M*–*T* curve, there were dual paramagnetic–ferromagnetic transitions and the mixed phase state.

The plot shown in Fig. 4 was the *M*–*H* loop for $La_{0.6}Pr_{0.1}Pb_{0.3}MnO_3$ sample, had been measured at three temperature scales (160 K, 220 K, and 275 K), the slope in the high field (tail) segment of *M*–*H* loop at 160 K was basically flattish with the ferromagnetic phase state; the slope in the tail segment of *M*–*H* loop at 220 K was feebly bended with the ferromagnetic, little paramagnetic mixed phase state; the slope in the high field segment of *M*–*H* loop at 275 K was visibly tilted with the ferromagnetic, some unturned paramagnetic mixed phase state.

The existence of paramagnetic, ferromagnetic, and insulating, metallic clusters in manganites $La_{0.6}Pr_{0.1}Pb_{0.3}MnO_3$ was likely originated from the synthetic preparation conditions, with dual-alternating or multi-alternating stacks of short and long Mn–O bonds from La, Pr, Mn, and O ions, implying distorted and undistorted $MnO_6$ octahedral clusters, which brought on dual Paramagnetic–Ferromagnetic transitions and the coexisting ferromagnetic, paramagnetic, insulating, and metallic mixed phase state characteristics on 200 K–320 K temperature segment [26,27,35–37].

Fig. 5 showed the plots of magnetization against applied field obtained at various temperatures for the sample of $La_{0.6}Pr_{0.1}Pb_{0.3}MnO_3$. In our experiments, the changing rate of applied field (20 Oe/s) was slow enough to get an isothermal *M*–*H* curve.

The entropy change, which results from the spin-ordering (i.e. ferromagnetic ordering) and is induced by the variation of the applied magnetic field from 0 to $H_{max}$, is given by

$$\Delta S_H = \int_0^{H_{max}} \left(\frac{\partial S}{\partial H}\right)_T \mathrm{d}H \tag{1}$$

From Maxwell's thermodynamic relation:

$$\left(\frac{\partial M}{\partial T}\right)_H = \left(\frac{\partial S}{\partial H}\right)_T, \tag{2}$$

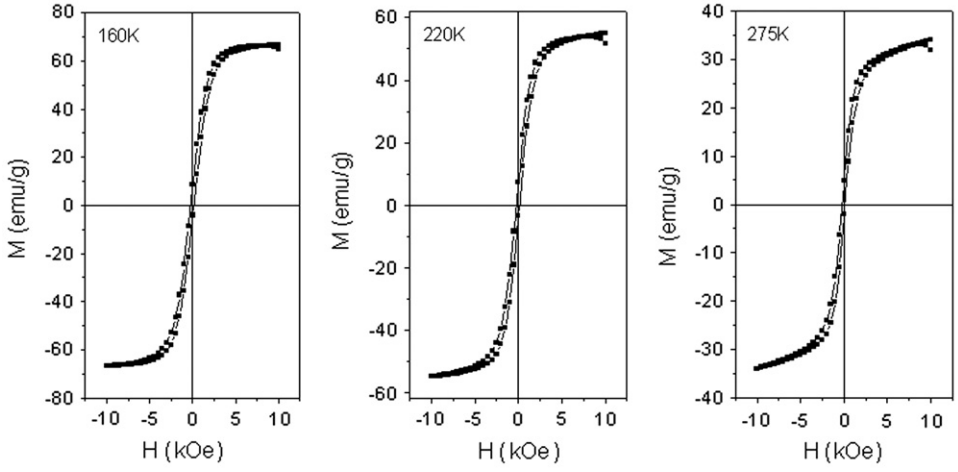


**Fig. 4.** Shows *M*–*H* loops at 160 K, 220 K, 275 K, respectively, for sample $La_{0.6}Pr_{0.1}Pb_{0.3}MnO_3$.

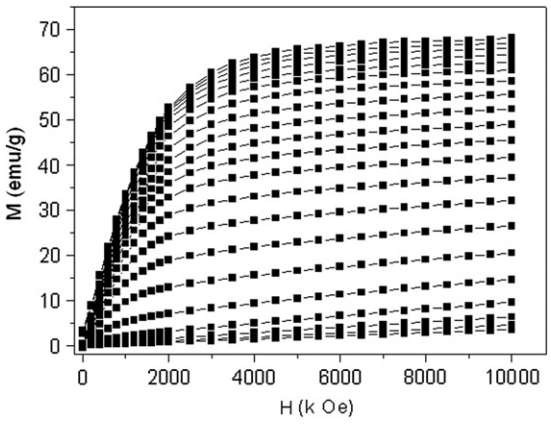


**Fig. 5.** Isothermal magnetizations of sample as a function of applied field at different temperature for $La_{0.6}Pr_{0.1}Pb_{0.3}MnO_3$. The temperature step is 10 K in the region near Curie temperature from 200 K to 350 K.

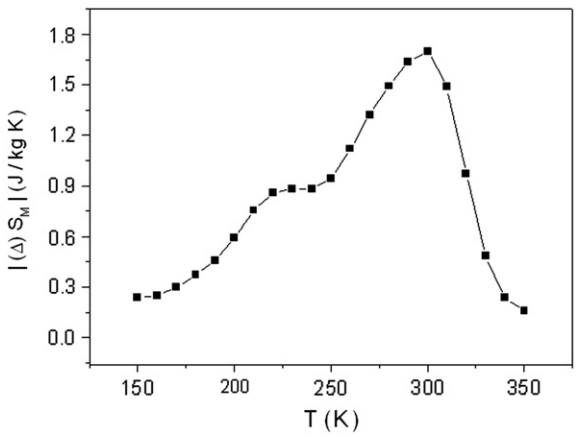


**Fig. 6.** Magnetic entropy changes of $La_{0.6}Pr_{0.1}Pb_{0.3}MnO_3$ sample at a magnetic field $H=10$ kOe as a function of temperature.

One can obtain the following expression:

$$\Delta S_H = \int_0^{H_{\max}} \left(\frac{\partial M}{\partial T}\right)_H \mathrm{d}H, \tag{3}$$

In the formula, $H_{\max}$ is the maximum external magnetic field. According to Eq. (3), the magnetic entropy change depends on the temperature-gradient of magnetization and attains a maximum value around Curie temperature $T_C$ at which the magnetization decays most rapidly.

In fact, the magnetic entropy change $\Delta S_H$ is often evaluated by some numerical approximation methods. One way of approximation is to directly use the measurements of $M$–$T$ curve under different magnetic fields. In the case of small discrete field intervals, $\Delta S_H$ can be approximated from Eq. (3) as

$$\Delta S_H = \sum_i \left[\left(\frac{\partial M}{\partial T}\right)_{H_i} + \left(\frac{\partial M}{\partial T}\right)_{H_{i+1}}\right] \times \frac{1}{2} \times \Delta H_i, \tag{4}$$

In the formula, $(\partial M/\partial T)_{H_i}$ is the experimental value obtained from $M$–$T$ curve in magnetic field $H_i$. Another method is to use isothermal magnetization measurements. In the case of magnetization measurements at small discrete field and temperature intervals, $\Delta S_H$ can be approximated from Eq. (3) by

$$\Delta S_H = \sum_i \frac{M_i - M_{i+1}}{T_{i+1} - T_i} \Delta H_i \tag{5}$$

In this paper, we adopt the latter method to evaluate the entropy change associated with applied field variation.

Fig. 6 showed the temperature dependence of magnetic entropy change for sample $La_{0.6}Pr_{0.1}Pb_{0.3}MnO_3$. As expected from Eq. (3), the peak of magnetic entropy changes of the sample was around Curie temperature $T_C$. It was clear that the magnetic entropy change in the series originates from the considerable change of magnetization near $T_C$. The maximum entropy change $\Delta S_H$ corresponding to a magnetic field variation of 10 kOe for $La_{0.6}Pr_{0.1}Pb_{0.3}MnO_3$ was about $-1.7$ J/kg K at 300 K.

From a cooling perspective, it is important to consider not only the magnitude of the magnetic entropy change but also the refrigerant capacity (RC), which depends on both the magnetic entropy change and its temperature dependence.

The magnetic cooling efficiency of a magnetocaloric material can be, in simple cases, evaluated by considering the magnitude of $\Delta S_H$ and its full-width at half maximum ($\delta T_{FWHM}$) [8,31,32]. It is easy to establish the product of the $\Delta S_H$ maximum and the full-width at half maximum ($\delta T_{FWHM} = T_2 - T_1$) as

$$RCP = -\Delta S_H(T,H) \times \delta T_{FWHM}$$

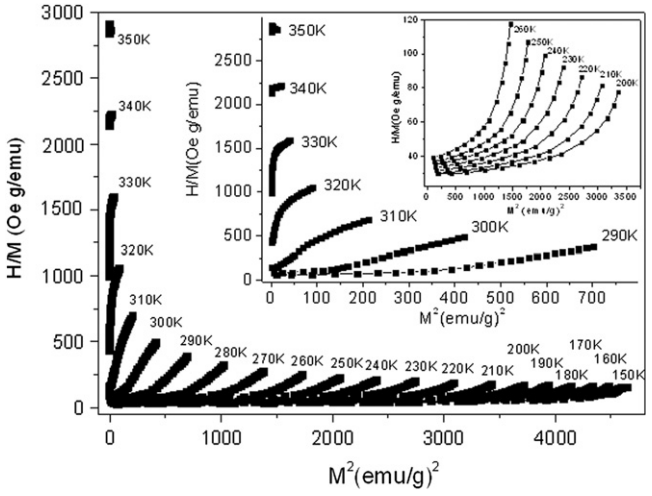


**Fig. 7.** $H/M$ vs $M^2$ plots of isotherms around Curie temperature, the biggish inset clearly showed that the slope of isotherm plots from the negative sign to the positive sign for 290 K–350 K temperatures, the lesser inset showed that the slope of isotherm plots in the unaltered positive sign for 200 K–260 K temperatures.

where stands for the so-called relative cooling power (*RCP*) based on the magnetic entropy change. In $La_{0.6}Pr_{0.1}Pb_{0.3}MnO_3$ sample, 170 J/kg *RCP* was figured out corresponding to a magnetic field variation of 10 kOe. In the accurately integral way cases, $RCP \approx 123.8$ J/kg.

To show physical characteristic of the first-order or second-order phase transition, one of the ways to determine is use of the Banerjee criteria in 1964 through analyzing $H/M$ vs $M^2$ curves, Banerjee detected the essential similarity between the Laudau-Lifshitz and Bean-Rodbell criteria and condensed them into one that provides a tool to distinguish first-order magnetic transitions from second-order ones by purely magnetic methods. It consists on the observation of the slope of isotherm plots of $H/M$ vs $M^2$. Fig. 7 was shown $H/M$ vs $M^2$ plots of Fig. 5 isotherms in the vicinity of the Curie temperature. It was clear that the biggish inset plots of Fig. 7 showed from the negative sign to the positive sign for some temperatures, which indicated that this phase transition was a first-order phase transition, contrast to the slope sign in the invariable positive that denoting the second-order character of the phase transition [33,34].

Temperature-dependent resistivity behavior of the samples showed obvious existence of double metal–insulator peaks, $T_{p1}$ and $T_{p2}$ for sample $La_{0.6}Pr_{0.1}Pb_{0.3}MnO_3$. However, the double peaks of the maximum magnetic entropy change, which is

expected according to the double peaks of the resistivity, were not manifested in this sample. Our results showed that $T_{p1}$, which coincides with $T_C$, was related to the DE mechanism as it was affected by external magnetic field and was also accompanied by a MR peak. $T_{p2}$ peak in $La_{0.6}Pr_{0.1}Pb_{0.3}MnO_3$ was likely originated from the synthetic preparation conditions, with dual-alternating or multi-alternating stacks of short and long Mn–O bonds from La, Pr, Mn and O ions, i.e. distorted and undistorted $MnO_6$ octahedral clusters, which brought on the coexisting of paramagnetic, ferromagnetic, and insulating, metallic clusters [35–37]. That the diagrams of magnetic entropy change vs temperature in external magnetic field was response of mixed magnetic inhomogeneity phase, the comparative faint magnetic signal from the Pr ions inhomogeneity existed in the octahedral frame submerged in the strong magnetic signal originated from the dominating octahedral frame both in the double exchange mechanism, and the magnetic entropy change counted by the differential coefficient of magnetic moment to temperature, so the double peaks of maximum magnetic entropy change had not occurred, but the width at half maximum in the magnetic entropy change comparatively broadened.

## Acknowledgements

The work was supported by National Laboratory of Solid State Microstructure of Nanjing University (LSSMS) under Grant no. M 23005, Department of Personnel Jiangsu Six Talent Fund under Grant no. AD 41118, and Top-Grade CNC Machine Tools and Basic Manufacture Projects under Grant no. 2010ZX04004-116.

## References

[1] A.J. Millis, Nature 392 (1998) 147.
[2] P.G. Radaelli, G. Iannone, M. Marezio, H.Y. Hwang, S.-W. Cheong, J.D. Jorgensen, D.N. Argyriou, Phys. Rev. B 56 (1997) 8265.
[3] H.Y. Hwang, S.-W. Cheong, P.G. Radaelli, M. Marezio, B. Batlogg, Phys. Rev. Lett. 75 (1995) 914.
[4] J. Fontcuberta, B. Martinez, A. Seffar, S. Pinol, J.L. Garcia-Munoz, X. Obradors, Phys. Rev. Lett. 76 (1996) 1122.
[5] H. Roder, Jun Zang, A.R. Bishop, Phys. Rev. Lett. 76 (1996) 1356.
[6] Z.B. Guo, Y.W. Du, J.S. Zhu, H. Huang, W.P. Ding, D. Feng, Phys. Rev. Lett. 78 (1997) 1142.
[7] E. Dagotto, T. Hotta, A. Moreo, Phys. Rep. 344 (2001) 1.
[8] M.H. Phan, S.C. Yu, J. Magn. Magn. Mater. 308 (2007) 325.
[9] C. Zener, Phys. Rev. 81 (1951) 440;
C. Zener, Phys. Rev. 82 (1951) (1951) 403.
[10] D.T. Morelli, A.M. Mance, J.V. Mantese, A.L. Micheli, J. Appl. Phys. 79 (1996) 373.
[11] Y. Sun, X.J. Xu, Y.H. Zhang, J. Magn. Magn. Mater 219 (2000) 183.
[12] X.X. Zhang, J. Tejada, Y. Xin, G.F. Sun, K.W. Wong, X. Bohigas, Appl. Phys. Lett. 69 (1996) 3596.
[13] W. Zhong, W. Chen, W.P. Ding, N. Zhang, A. Hu, Y.W. Du, Q.J. Yan, J. Magn. Magn. Mater 195 (1999) 112.
[14] X. Bohigas, J. Tejada, M.L. Marinez-Sarrion, S. Ttipp, R. Black, J. Magn. Magn. Mater 208 (2000) 85.
[15] J. Mira, J. Rivas, L.E. Hueso, F. Rivadulla, M.A. Lopez Quintela, J. Appl. Phys. 91 (2002) 8903.
[16] S.M. Yusuf, J.M. De Teresa, P.A. Algarabel, J. Blasco, M.R. Ibarra, Amit Kumar, C Ritter, Physica B 385–386 (2006) 401.
[17] B.F. Yu, Q. Gao, B. Zhang, X.Z. Meng, Z. Chen, Int. J. Refrig 26 (2003) 622.
[18] Qianying Yu, Jincang Zhang, Rongrong Jia, Chao Jing, Shixun Cao, J. Magn. Magn. Mater 320 (2008) 3313.
[19] M. Mazaheri, M. Akhavan, Physica B 405 (2010) 72.
[20] Y. Moritomo, H. Kuwahara, Y. Tomioka, Y. Tokura, Phys. Rev. B 55 (1997) 7549.
[21] M. Kumaresavanji, M.S. Reis, Y.T. Xing, M.B. Fontes, J. Phys. Conf. Ser. 200 (2010) 052013.
[22] K. Mydeen, S. Arumugam, D. Prabhakaran, R.C. Yu, C.Q. Jin, J. Alloys Compd 468 (2009) 280.
[23] N. Ibrahim, A.K. Yahya, S.S. Rajput, S. Keshri, M.K. Talari, J. Magn. Magn. Mater. 323 (2011) 2179.
[24] M. Uehara, S. Mori, C.H. Chen, S.-W. Cheong, Nature 399 (1999) 560.
[25] M. Fath, S. Freisem, A.A. Menovsky, Y. Tomioka, J. Aarts, J.A. Mydosh, Science 285 (1999) 1540.
[26] S.J.L. Billinge, Th. Proffen, V. Petkov, J.L. Sarrao, S. Kycia, Phys. Rev. B 62 (2000) 1203.
[27] E. Dagotto, T. Hotta, A. Moreo, Phys. Rep 344 (2001) 1.
[28] G.N Rao, R.C SaibalRoy, Yang, J.W. Chen, J. Magn. Magn. Mater. 260 (2003) 375.
[29] G.H. Zheng, Z.X. Dai, Y.Y. Zhang, Y.P. Sun, J. Alloys Compd. 489 (2010) 348.
[30] Shiming Zhou, Lei Shi, Jiyin Zhao, Haipeng Yang, Lin Chen, Solid State Commun 142 (2007) 634.
[31] V.K. Pecharsky, K.A. Gschneidner, A.O. Tsokol, Rep. Prog. Phys. 68 (2005) 1479.
[32] V.K. Pecharsky, K.A. Gschneidner, Annu. Rev. Mater. Sci. 30 (2000) 387.
[33] B.K. Banerjee, Phys. Lett. 12 (1964) 16.
[34] J. Mira, J. Rivas, F. Rivadulla, C. Vazquez-Vazquez, M.A. Lopez-Quintela, Phys. Rev. B 60 (1999) 2998.
[35] M.C. Kao, H.Z. Chen, S.L. Young, C.Y. Shen, L. Horng, J. Alloys Compd 440 (2007) 18.
[36] A. Moreo, S. Yunoki, E. Dagotto, Science 283 (1999) 26.
[37] P.G. Radaelli, G. Iannone, M. Marezio, H.Y. Hwang, S.-W. Cheong, J.D. Jorgensen, D.N. Argyriou, Phys. Rev. B 56 (1997) 8265.